Event-driven Brownian dynamics for hard spheres

A. Scala
Dipartimento di Fisica, Universitá di Roma "La Sapienza," Piazzale Aldo Moro 2, 00185 Roma, Italy and INFM-CRS SMC, Universitá di Roma "La Sapienza," Piazzale Aldo Moro 2, 00185 Roma, Italy

Th. Voigtmann
Scottish Universities Physics Alliance, School of Physics, The University of Edinburgh, JCMB King's Buildings, Edinburgh EH9 3JZ, United Kingdom

C. De Michele
Dipartimento di Fisica, Universitá di Roma "La Sapienza," Piazzale Aldo Moro 2, 00185 Roma, Italy and INFM-CRS SOFT, Universitá di Roma "La Sapienza," Piazzale Aldo Moro 2, 00185 Roma, Italy

(Received 30 June 2006; accepted 1 March 2007; published online 4 April 2007)

Brownian dynamics algorithms integrate Langevin equations numerically and allow to probe long time scales in simulations. A common requirement for such algorithms is that interactions in the system should vary little during an integration time step; therefore, computational efficiency worsens as the interactions become steeper. In the extreme case of hard-body interactions, standard numerical integrators become ill defined. Several approximate schemes have been invented to handle such cases, but little emphasis has been placed on testing the correctness of the integration scheme. Starting from the two-body Smoluchowski equation, the authors discuss a general method for the overdamped Brownian dynamics of hard spheres, recently developed by one of the authors. They test the accuracy of the algorithm and demonstrate its convergence for a number of analytically tractable test cases. © *2007 American Institute of Physics*. [DOI: 10.1063/1.2719190]

I. INTRODUCTION

The simulation of interacting Brownian particles, called Brownian dynamics (BD) simulation,[1] has become an important tool in condensed matter, colloidal, and biological physics. In particular at high densities, the excluded volume has a major effect on the dynamics of the Brownian particles. Consequently, many model colloids are well described by effective pair interactions that are hard-sphere (HS)-like, or have a HS core with additional potential tails. This places the hard-sphere system (with or without random "Brownian" forces) among the most important reference systems for the theories in the field.[2,3] However, such theories are in general only approximate, requiring extensive testing through experiment and computer simulation. Yet, the simulation of hard spheres with Brownian dynamics is not straightforward, because of the singular nature of the interaction potential: most methods dealing with the numerical integration of stochastic differential equations (SDEs) require a certain degree of smoothness in all the interactions.

Several hard-core BD algorithms have been proposed and applied in the past,[4–10] with a varying degree of justification. Our aim here is to discuss a novel approach developed by one of us,[11] called De Michele's algorithm in the following. We investigate the convergence to the true solutions of the singular SDE by studying special situations where the theoretical behavior is under control, in order to validate the correctness of the approach. This is the first step in a program to extend De Michele's algorithm to more complicated cases, such as taking into account inertial effects (negligible by assumption in BD), or more complicated singular interactions.

Of course the hard-sphere potential [$\beta V(r)=\infty$ if two particles overlap, zero otherwise, where $\beta=1/(k_BT)$ is the inverse temperature] is a purely theoretical concept. One may view steeply repulsive "soft-sphere" potentials, e.g., $V(r)\propto r^{-n}$ with large n, as more convenient model systems for colloids,[5,12] and try to infer HS ($n\to\infty$) behavior by extrapolating n or by a suitable mapping of finite-n results to proper HS dynamics, which requires additional structural information.[12,13] Unless this is done, the $n\to\infty$ extrapolation forces such soft-sphere methods to use rather small integration time steps, in order to ensure that forces vary little during any such step. In our view, a proper HS-BD algorithm which circumvents extrapolation or mapping procedures is desirable.

We will not discuss hydrodynamic interactions (HI), i.e., the solvent-induced interactions that are present in typical experimental realizations of Brownian systems. Taking them into account properly would ensure that hard spheres do not overlap, due to divergent lubrication forces.[14] To deal with HI, several computational methods have been developed, for example, Stokesian dynamics,[15] lattice Boltzmann simulations,[16–19] dissipative particle dynamics,[20,21] or fluid particle methods.[22] Usually they either deal with softened interactions again and/or are rather time consuming; depending on the method, a huge number of degrees of freedom needs to be considered, or the intricate nature of the non-pairwise-additive long-range HI forces the use of elaborate

schemes. While the theory of HI is well understood at low particle densities, much less is known at high densities, and theories often proceed by claiming them irrelevant. A non-HI simulation therefore has its place in testing such theories, and in circumventing the huge effort of the HI methods, should the claim be true.

Testing the goodness of the approximations inherent to all existing HS-BD algorithms has up to now received little attention. One needs to test properties that are inherent both to the Brownian dynamics of the system and to the hard-core collisions. Testing for diffusive behavior is obviously not enough, in as far as at high densities and long times it is related to the chaotic nature of the many-body problem and not to the details of the implemented equation of motion or its correctness. In some previous work, static quantities such as the radial distribution function $g(r)$ have been checked;[9] such comparisons do not test whether a HS-BD algorithm properly discretizes the Langevin SDE, but rather its ergodicity.

We will therefore discuss tests of BD-HS algorithms that involve probing the hard-sphere interactions but still allow for a comparison with exact results known for the Brownian system, i.e., where the Langevin equation can be solved exactly in terms of a time-dependent probability distribution function (PDF). In such a case, an empirical PDF can be generated from sufficiently many runs of the algorithm in question and then be compared to the exact solution.

The method we are going to discuss in the present paper is a crossbreed between standard Brownian methods (ignoring the singular potential) and the standard event-driven (ED) simulation method for the ordinary (nonstochastic) dynamics of hard spheres. Predecessors date back to Monte Carlo (MC) inspired schemes,[4–8] culminating in the algorithm by Strating[9] and algorithms making use of so-called overlap potentials.[23] Strating's algorithm is but a step away from De Michele's algorithm[11] investigated here. A slightly different principle has also recently been implemented by Tao *et al.*,[10] albeit applied to a more complex system of hard rods. We will discuss both these ED-BD methods, with an emphasis on De Michele's algorithm, which we will show to be exact to first order in the integration-step size Δt.

Our algorithm is different from the other HS-BD methods mentioned, a variant of the hybrid Monte Carlo[24,25] (HMC) scheme, as well shall detail below. This grants the property that it reproduces correctly the static properties of the HS system.

This paper is organized as follows: the next section discusses the theoretical background, Sec. III introduces the idea of ED-BD and De Michele's algorithm (extending it to the case of linear shear flows and constant external forces). Section IV demonstrates its convergence to the BD-PDF on the two-body level, while Sec. V focuses on a comparison of the algorithm's many-body behavior with the theoretical predictions. Section VI summarizes and concludes.

II. HARD-SPHERE BROWNIAN DYNAMICS ALGORITHMS

We start from the N-particle ($1 \leqslant i \leqslant N$) Langevin equation

$$m_i \dot{\mathbf{v}}_i = \mathbf{f}_i^p + \mathbf{f}_i^r + \mathbf{f}_i^d + \mathbf{f}_i^{\mathrm{ext}}, \tag{1}$$

where the subscripts i label the particles and will be dropped where they are clear from the context. In Eq. (1), $\mathbf{f}^p$ incorporates the effect of the HS interaction and $\mathbf{f}^{\mathrm{ext}}$ is a sufficiently smooth external force. $\mathbf{f}^r$ and $\mathbf{f}^d$ are the random and dissipative forces resulting in Brownian dynamics, therefore the above equation is a second-order SDE in the particle positions. The random force is characterized by its zero mean and the correlation

$$\langle \mathbf{f}^r(t) \otimes \mathbf{f}^r(t') \rangle = 2k_B T \boldsymbol{R}\, \delta(t-t'). \tag{2}$$

The fluctuation-dissipation theorem (FDT) then requires the dissipation to be $\mathbf{f}^d = -\boldsymbol{R}(\mathbf{v}-\mathbf{u})$, where $\mathbf{u}$ is a local flow velocity field; $\mathbf{u}$ is nonzero in the case of applied shear, $\mathbf{u} = \dot{\boldsymbol{\Gamma}}\mathbf{r}$, where $\dot{\boldsymbol{\Gamma}}$ is a shear-rate tensor. $\boldsymbol{R}$ is in general a complicated matrix depending on the full configuration of the system at any given time, representing HI. Here we are concerned with the simpler case where $\boldsymbol{R} = \xi \mathbf{1}$ is constant, with a real number $\xi > 0$. In this paper we furthermore deal with the limit $m/\xi \to 0$, the case of strong dissipation, where Eq. (1) reduces to a first-order SDE in the positions,

$$\xi \mathbf{v} = \mathbf{f}_i^p + \mathbf{f}_i^r + \xi \mathbf{u} + \mathbf{f}_i^{\mathrm{ext}}. \tag{3}$$

In what follows, we will, according to customary procedure,[26] assume that one can fix a small enough time interval Δt over which the particle configuration and all smooth forces vary slowly, allowing them to be treated as constant. If this were possible for $\mathbf{f}^p$ as well, one could use conventional SDE integrators,[27] a topic in its own right (see, e.g., Refs. 1 and 28–36). For hard spheres, the forces are not Lipschitz continuous and standard numerical integrators are ill defined.[37] Integrating Eq. (3) over the interval Δt, one obtains

$$\Delta \mathbf{r}(\Delta t) = \mathbf{g} \Delta t + \boldsymbol{\mu}(\Delta t), \tag{4}$$

where $\mathbf{g} = \mathbf{u} + \xi^{-1}(\mathbf{f}^p + \mathbf{f}^{\mathrm{ext}})$ contains the systematic and interaction terms, while $\boldsymbol{\mu}$ is a Wiener process with $\langle \boldsymbol{\mu}(t) \otimes \boldsymbol{\mu}(t') \rangle = 2\boldsymbol{D} \min(t,t')$, where $\boldsymbol{D} = k_B T \boldsymbol{R}^{-1T} = (k_B T/\xi)\mathbf{1}$ is the matrix of diffusion coefficients. Note that we still allow these bare diffusion coefficients to depend on the particle index, as it may arise in multicomponent (polydisperse) systems.

We discuss the case $\mathbf{u} = \mathbf{f}^{\mathrm{ext}} = 0$ first. One approach is to simply set $\mathbf{f}^p = 0$ in generating random displacements $\Delta \mathbf{r}$ with the statistics given by $\boldsymbol{\mu}$.[4–9] A second step then is needed to ensure that the random displacements are compatible with the presence of $\mathbf{f}^p \neq 0$; for hard spheres this is the criterion that no two particles overlap. One can either discard all displacements that violate this condition—this is a variant of standard Metropolis MC (called simply MC in the following). It has been shown[4] that in the limit $\Delta t \to 0$ one indeed obtains Brownian dynamics, i.e., a faithful realization of Eq. (3). We will discuss this point again further on.

More elaborate overlap removal can be applied: some implementations put particles back at contact (or around contact on average) along the line of their relative displacement,[5–8] although this has unwanted effects on the pair distribution function, hence on observable such as pressure. Strating[9] proposed to remove overlaps by performing

elastic collisions: from the time step Δt and the displacement $\Delta \mathbf{r}$, assign a fictive velocity $\mathbf{v}=\Delta \mathbf{r}/\Delta t$ to the particles, and move them by displacements $\Delta \mathbf{r}$ as if they underwent ballistic flight (including eventual elastic collisions) with this velocity $\mathbf{v}$ in the time interval Δt.

Whatever the removal procedure (other than simple rejection), one has to be aware that the removal of one overlap can itself create new (called secondary, tertiary, and so forth) overlaps. This is especially likely to happen in dense systems. As Strating pointed out, both the removal of all these "higher-order" overlaps as well as the order in which overlaps are removed are crucial for the algorithm to work. According to Ref. 9, one needs to remove them in the order in which they would have occurred in a Newtonian-dynamics simulation.

At this point it is convenient to turn around the discussion and start from an algorithm that treats Eq. (3) in the opposite limit: If ξ were zero, one would recover the standard Newtonian dynamics of hard spheres. The best numerical schemes in this case are ED simulations:[38,39] assuming the collisions are binary in all nondegenerate cases and of infinitesimal duration, one advances the system from one such collision to the next, solving the intermediate ballistic-free flight exactly. The random force in Eq. (3) prevents a naive application of this approach, but we can reintroduce randomness as follows: if we interpret the velocities of the ED simulation as the fictive velocities of the above discussion, randomly drawn every Δt, the ED scheme is simply a device to prevent all unphysical overlaps in the first place, using a set of vectors $\mathbf{v}$ as its book-keeping device.

Note that in terms of efficiency, there is little difference to Strating's method, since the main effort in ED simulation goes into the calculation and the sorting of collision times, something that is also needed when one is to remove overlaps in their "correct" order. Note also that this algorithm bears a resemblance to some ED granular matter simulations,[40–44] where, however, a modified kinetic equation instead of Eq. (1) needs to be solved.

The question then arises how to interpret and perform "Brownian collisions" in such a combined ED-BD scheme. We will argue below that the elastic collision rule of Newtonian dynamics is a reasonable choice, inspired by its exactness in one dimension. This is De Michele's algorithm, first used in Ref. 11. In the limit of small Δt and for vanishing $\mathbf{u}$ it is essentially Strating's algorithm, with the overlap problem cured. (For large Δt, the two algorithms differ in the treatment of one particle "tunneling" across another.) We also discuss another choice, made by Tao *et al.*[10] in the more complicated context of hard rods: instead of ballistic collisions, where the pre- and postcollision velocities are perfectly correlated, one can decorrelate them by assigning the postcollision velocity randomly (with proper restrictions to avoid overlaps).

III. EVENT-DRIVEN BROWNIAN DYNAMICS

A. The Brownian two-body problem

To investigate the role of ED collisions in the BD algorithm, we study the two-body BD-HS problem without external forces in more detail. This can be solved analytically[45,46] by transforming from the particle coordinates $\mathbf{r}_i, i=1,2$, to the relative $\mathbf{r}=\mathbf{r}_1-\mathbf{r}_2$ and center-of-motion coordinates $\mathbf{R}=\Xi^{-1}(\xi_1\mathbf{r}_1+\xi_2\mathbf{r}_2)$, where $\Xi=\xi_1+\xi_2$. The latter then separates from the problem, giving free center-of-motion diffusion. In the relative coordinates, the hard-core interactions can be included as a boundary condition into the diffusion equation of a point particle,

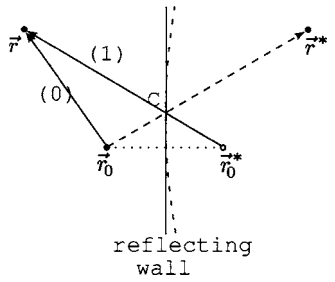

FIG. 1. Illustration of the image-method treatment of "Brownian collisions" in De Michele's algorithm. The probability of moving one particle from $\mathbf{r}_0$ to $\mathbf{r}$ in a time step Δt is the sum of the direct part (0) and a part (1) corresponding to the transition from the image $\mathbf{r}_0$ of the starting point with respect to the wall (vertical solid line) to the final $\mathbf{r}$. The latter occurs with probability equal to that of a move from $\mathbf{r}_0$ to $\mathbf{r}^*$ (the image of $\mathbf{r}$) and is simulated by reflecting such a trajectory at the wall (point C). The dashed circular arc indicates the typical dimension of the real hard-sphere boundary in the $\mathbf{r}_0-\mathbf{r}$ plane for realistic parameters (average $\Delta r \approx 0.1\sigma$).

$$\partial_t p(\mathbf{r},t) = D\nabla^2 p(\mathbf{r},t), \quad r > \sigma, \tag{5a}$$

$$\mathbf{r}\cdot\nabla p(\mathbf{r},t) = 0, \quad r = \sigma, \tag{5b}$$

where $p(\mathbf{r},t)$ is the PDF for finding a relative distance $\mathbf{r}$ at time t, $D=D_1+D_2$ is the relative diffusion coefficient, and $\sigma=(\sigma_1+\sigma_2)/2$ with the particle diameters σ_i.

One could aim to include the exact solution of this case in a HS-BD algorithm by drawing particle displacements according to this $p(\mathbf{r},t)$ whenever two particles are sufficiently near. However, the procedure would be rather involved, since the analytical solution[45,46] is only available as an infinite sum in the Laplace domain. It would also be only approximate in the presence of more than two particles, hence valid only for small time steps, and more gravely, again introduce secondary-overlap problems.

It is therefore easier to consider the limit of small Δt, then, the interaction between HS particles only becomes relevant for small $r-\sigma$. In this limit, the boundary at $r=\sigma$ can be considered as flat and the analytical PDF can be easily obtained by the method of images. Denoting by $G_0(\mathbf{r},t_0+\Delta t|\mathbf{r}_0,t_0)$ the Green's function of the unbounded diffusion equation (for a particle starting at $\mathbf{r}_0$ at time t_0), we then have[47]

$$p(\mathbf{r},t_0+\Delta t|\mathbf{r}_0,t_0) = G_0(\mathbf{r},t_0+\Delta t|\mathbf{r}_0,t_0) + G_0(\mathbf{r},t_0+\Delta t|\mathbf{r}_0^*,t_0) \tag{6}$$

for $r>\sigma$, and zero otherwise. Here, $\mathbf{r}_0^*$ is the mirror image of the initial coordinate $\mathbf{r}_0$ with respect to the boundary. A well-known simple geometrical transformation, illustrated in Fig. 1, relates $p(\mathbf{r},t_0+\Delta t|\mathbf{r}_0,t_0)$ to the free $G_0(\mathbf{r},t_0+\Delta t|\mathbf{r}_0,t_0)$: starting from $\mathbf{r}_0$, extract a new position $\mathbf{r}^*$ according to G_0 and accept it ($\mathbf{r}=\mathbf{r}^*$) if moving from $\mathbf{r}_0$ to $\mathbf{r}^*$ does not cross

the boundary. Otherwise, if the extracted transition from $\mathbf{r}_0$ to $\mathbf{r}^*$ crosses the boundary, update $\mathbf{r}^* \mapsto \mathbf{r}$ by reflecting it at the boundary. The resulting $\mathbf{r}$ arises from the direct contribution (left-hand arrow) and the reflected one, where the latter has the same probability as a transition from $\mathbf{r}_0^*$, the mirror image of $\mathbf{r}_0$, to $\mathbf{r}$. Hence the endpoints $\mathbf{r}$ are distributed according to p. The reflection of $\mathbf{r}^*$ is equivalent to a "ballistic" collision of the trajectory at the boundary (point marked C in the figure) if one uses a fictive velocity $\mathbf{v}=\Delta\mathbf{r}/\Delta t$ in the process.

Transforming back to the individual particles' coordinates, an algorithm implementing the above geometrical construction runs as follows: during the time interval Δt, perform ballistic flights for both particles, with fictive velocities $\mathbf{v}$ chosen from a probability distribution $f(\mathbf{v})$ that satisfies $f(\mathbf{v}=\Delta\mathbf{r}/\Delta t)d\mathbf{v}=G_0(\Delta\mathbf{r},t_0+\Delta t|0,t_0)d\mathbf{r}$. This will satisfy the correct diffusion equation for the above no-flux boundary conditions, as long as the correct solution can be obtained by the image method and G_0 describes a homogeneous process, i.e., depends on position only through the difference $\Delta\mathbf{r}=\mathbf{r}-\mathbf{r}_0$, and not on $\mathbf{r}$ and $\mathbf{r}_0$ individually. More generally, it will implement the correct boundary conditions if Δt is chosen small enough such that in every time interval and for almost all cases, the reflection procedure applies only when $r_0-\sigma$ is sufficiently small to consider the boundary as flat.

The fictive-velocity distribution corresponding to free Brownian diffusion, $G_0(\Delta\mathbf{r},\Delta t)=(4\pi D\Delta t)^{-d/2}\exp[-(\Delta\mathbf{r})^2/(4D\Delta t)]$, is of course just the Maxwell-Boltzmann distribution, $f(v)=(\beta m/2\pi)^{-d/2}\exp[-\beta(m/2)v^2]$. This connection is essentially the way in which the FDT enters the ED-BD algorithms. The parameter βm_i sets the bare diffusion coefficient for each particle i, given as

$$D_i=\frac{\Delta t}{2}\frac{1}{\beta m_i}. \tag{7}$$

In particular, polydisperse systems, where different HS species have different D_i, can be simulated by incorporating elastic collisions according to the (fictive) masses m_i.

B. The many-body algorithm

De Michele's ED-BD algorithm[11] for hard spheres applies the above two-body approach to the case of many particles:

(i) every $t_n=n\Delta t$ (n integer) extract velocities $\mathbf{v}_i$ according to a Maxwellian distribution with fictive masses obeying Eq. (7);
(ii) evolve the system between t_n and $t_n+\Delta t$ according to the laws of ballistic motion (performing ED molecular dynamics).

In other words, Gaussian particle displacements $\Delta\mathbf{r}_i=\mathbf{v}_i\Delta t$ are extracted according to $\langle\Delta\mathbf{r}_i^2\rangle=2dD_i\Delta t$ (in d dimensions) and ED rules enforce no-flux boundary conditions at the particle surfaces.

There are two central approximations inherent in this algorithm: one is due to the fact that the image method cannot be used to construct the exact two-body PDF for two Brownian hard spheres. The approximation is indicated in Fig. 1, where the dashed circular arc represents the correct position of the two-body HS boundary, which the algorithm effectively replaces with the flat reflecting wall shown as the vertical solid line (depending on the angles of $\mathbf{r}_0$ and $\mathbf{r}$ with respect to the line joining the particle centers). Both approximations limit the maximum allowable time step Δt for the algorithm: the first requires $\Delta t \ll d_{\mathrm{avg}}^2/(4D)$, where $d_{\mathrm{avg}} \sim \rho^{-1/d}$ is a typical interparticle separation; the second requires $\Delta t \ll \sigma^2/(4D)$. In the limit $\Delta t \to 0$ the ED-BD algorithm converges to the correct solution, essentially since the boundary problem reduces to the one-dimensional case where the algorithm is exact. This statement will be made more precise in the following.

The possible occurrence of multiple collisions per time step poses another approximation within the algorithm. Its effect, however, is less severe: if we consider an arrangement of three instead of just two particles, multiple collisions essentially mimic a many-images solution for the Green's function of a point source (one moving particle) in a corner or wedge formed by the approximately planar surfaces of two other particles nearby. Such a solution will be sufficiently close to the real solution, in the spirit of treating three-particle (and higher) PDFs by a dynamical superposition approximation. The influence of this latter aspect is hard to quantify, but can be expected to become small in the small-Δt limit. In general, one expects that for small Δt, the N-body Smoluchowski operator can be decomposed in a leading two-body term, and smaller contributions from the higher-order correlations. That such a decomposition holds not only for low densities, but also for *short times* at high densities, was pointed out by Lionberger and Russel.[48] This argument lends justification to the use of our algorithm at high densities, where of course hard-sphere simulations become most interesting.

De Michele's algorithm essentially is a special case of the HMC scheme.[24,25] There, one combines the steps (i) and (ii) above with an acceptance criterion for each substep Δt. The acceptance rate is $\min(1,\exp[-\beta\delta\mathcal{H}])$ and differs from unity only when there is a non-negligible error $\delta\mathcal{H}$ in the total energy stemming from the numerical treatment of complicated Hamiltonians. For the ED simulation of a HS system, $\delta H \approx 0$ to machine precision, so that there is no difference between HMC and our ED-BD scheme. Incidentally, this equivalence makes clear that De Michele's algorithm explores phase space according to the canonical ensemble, as the corresponding proof for HMC can be directly transferred. Note that the equivalence is based crucially on the fact that within each subinterval Δt, we perform a Newtonian-dynamics simulation. The HMC properties are not granted, e.g., for Strating's method or the Tao-BD algorithm.

De Michele's algorithm can be extended in a straightforward manner to include a linear shear field, $\mathbf{u}=\dot{\Gamma}\mathbf{r}$, and external forces that change slowly in space (such that they can be approximated as constant over the typical Δr resulting in a time step). Let us discuss the case of linear shear flow in more detail. In this case one needs to deal with *two* effects on the Brownian motion: there will be a systematic drift $\mathbf{u}$, but also the noise term for Δr will be modified because $\mathbf{u}$

depends on $\mathbf{r}$. If the shear flow acts along the x direction, $\mathbf{u}=\dot{\gamma}y\mathbf{e}_x$, we have[49] $\langle\Delta y\rangle=\langle\Delta z\rangle=0$, $\langle\Delta x\rangle=y\dot{\gamma}\Delta t$, and $\langle\Delta y^2\rangle=\langle\Delta z^2\rangle=2D\Delta t$, but $\langle\Delta x^2\rangle=\langle\Delta x\rangle^2+2D\Delta t(1-(1/3)(\dot{\gamma}\Delta t)^2)$. The random displacements appearing in Eq. (4) in the presence of linear shear are also cross correlated, $\langle\Delta x\Delta y\rangle=(D\Delta t)(\dot{\gamma}\Delta t)$.

This leads to the following extension of De Michele's algorithm:

(i) extract random velocities $\mathbf{v}=(\Delta\mathbf{r}-\langle\Delta\mathbf{r}\rangle)/\Delta t$ from a multivariate Gaussian distribution according to the above averages;
(ii) add to the fictive velocities the systematic drift $\langle\Delta\mathbf{r}\rangle/\Delta t$ induced by the shear flow and/or gravity.

In previous applications of HS-BD algorithms to sheared systems, only the systematic drift has been taken into account (cf. Ref. 9). The effect of neglecting these high-shear-rate corrections to the Brownian displacements has not been studied so far and remains to be clarified. For constant external forces (such as gravity), only a systematic drift needs to be taken into account.

IV. TWO-BODY TESTS

As in two (and higher) dimensions, no exact solution in terms of a mirror image exists for the two-body HS problem, De Michele's algorithm even for two particles introduces an approximation which is worthwhile testing. We will first focus on the comparison of the single step PDF from various algorithms to the exact results, then to some checks of the convergence of the PDF after several steps.

A. Single-step behavior

The Laplace transform of the exact two-body distribution function in up to three dimensions has been given by Hanna *et al.*[45] and by Ackerson and Fleishman.[46] In two dimensions, for example, the relative part solving Eq. (5) is written with the Laplace frequency $s=D^2q^2$ and polar coordinates (r,φ),

$$p(r,\varphi,s|r_0,\varphi_0)=\frac{1}{2\pi D}\times\sum_m\left\{e^{im(\varphi-\varphi_0)}K_m(qr_>)I_m(qr_<)-e^{im(\varphi-\varphi_0)}K_m(qr_>)K_m(qr_<)\frac{I_m'(q\sigma)}{K_m'(q\sigma)}\right\},\tag{8}$$

where $r_>$ is the greater of r, r_0, and $r_<$ the lesser. $I_m(z)$ and $K_m(z)$ are the modified Bessel functions of the first and second kind of order m. (Here and in the following, D denotes the *relative* diffusion coefficient for the two-body problem.) This is to be contrasted with the two-body PDF implemented through the algorithm, i.e., the Laplace transform of Eq. (6). Using the addition theorem for the modified Bessel functions,[50]

$$p_{\mathrm{ED}}(r,\varphi,s|r_0,\varphi_0)=\frac{1}{2\pi D}\times\sum_m\{e^{im(\varphi-\varphi_0)}K_m(qr_>)I_m(qr_<)-e^{im(\varphi-\varphi_0^*)}K_m(qr_>^*)I_m(qr_<^*)\},\tag{9}$$

where (r_0^*,φ_0^*) are the polar coordinates of the mirror image, themselves complicated functions of (r_0,φ_0). The first term in the brackets is identical to the one in the correct solution and represents free diffusion. To show that the algorithm recovers the correct two-body case for small time steps, we analyze the second term in the limit $q\sigma\to\infty$. The second contribution in Eq. (8) then approaches $K_m(qr)K_m(qr_0)\exp[2q\sigma]\exp[im(\varphi-\varphi_0)]/\pi$ for not too large m (note that large orders of m are suppressed). On the other hand, the corresponding term in Eq. (9) approaches $K_m(qr_>^*)K_m(qr_<^*)\exp[2qr_<^*]\exp[im(\varphi-\varphi_0^*)]/\pi$. This agrees with the exact result in the further limit $r_0\to\sigma$, where by construction $\varphi_0^*\to\varphi$ and $r_0^*\to r_0$. For $r_0\gg\sigma$, the leading asymptote of both expressions is free diffusion. Therefore De Michele's algorithm converges to the correct BD result for $q\sigma\to\infty$ (corresponding to $D\Delta t/\sigma^2\ll1$). In three dimensions, the discussion proceeds along the sames lines, replacing the angular exponential and the Bessel functions with their spherical counterparts.

To discuss the influence of different initial separations r_0 more clearly, let us proceed by looking at a particular average that can be calculated exactly: the average displacement magnitude $|\langle\Delta\mathbf{r}\rangle_{dD}|=(\Sigma_i\langle\Delta x_i\rangle_{dD}^2)^{1/2}$, where x_i label the Cartesian components and $\langle\Delta x_i\rangle_{dD}=\int_{r>\sigma}r^{d-1}drd\Omega_d\Delta x_i p(\mathbf{r},s|\mathbf{r}_0)$ is the d-dimensional average, evaluates to a relatively simple expression whose inverse Laplace transform can be performed numerically.[51] In particular, noting $r_0>\sigma$,

$$\langle r\rangle_{1\mathrm{D}}=\frac{1}{q^3}e^{-q(r_0-\sigma)},\tag{10}$$

$$|\langle\mathbf{r}\rangle_{2\mathrm{D}}|=\left|\mathrm{LT}^{-1}\left[\frac{1}{q^3}\frac{K_1(qr_0)}{K_1'(q\sigma)}\right]\right|,\tag{11}$$

$$|\langle\mathbf{r}\rangle_{3\mathrm{D}}|=\left|\mathrm{LT}^{-1}\left[\frac{1}{q^3}\frac{k_1(qr_0)}{k_1'(q\sigma)}\right]\right|.\tag{12}$$

Both the two- and three-dimensional expressions, Eqs. (11) and (12), have the one-dimensional (1D) result, Eq. (10), as their leading asymptote for $q\to\infty$. This reconfirms that in the limit of small step sizes, the dynamics is governed by its one-dimensional equivalent, and that the ED-BD algorithm, providing this leading asymptote, converges as $\Delta t\to0$. To demonstrate the convergence behavior for small but finite Δt, we compare the exact result for the two-dimensional mean displacement, Eq. (11), with simulation data in Fig. 2. Each data point in the figure corresponds to an average over 50 000 runs starting from a given (x_0,y_0), each performing one step of size Δt as indicated in the different panels of the figure. Here and in the following, we choose units such that $\sigma=1$. The size of the time step shall be measured relative to the intrinsic "thermal" time $\beta m\sigma^2$.

De Michele's algorithm (circles) and Starting's algorithm (diamonds) give almost identical results for small

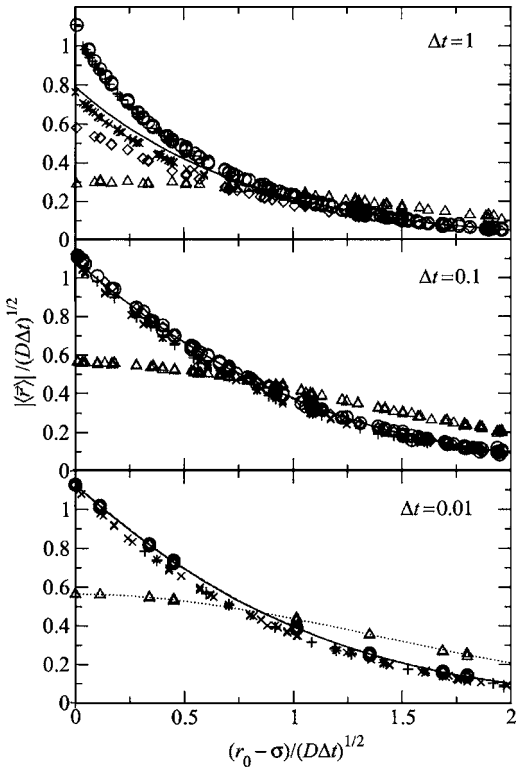

FIG. 2. Average displacement size, $|\langle \Delta \mathbf{r} \rangle_{2D}|$, for the two-dimensional Brownian motion of two equal hard spheres ($\sigma=1$) in their relative-coordinate frame; r_0 is the initial center-to-center distance. The relative diffusion coefficient is $D=\Delta t/2$; the step size Δt is kept fixed within each panel. All values are scaled by $1/\sqrt{D\Delta t}$. Symbols are one-time-step simulation results, averaged over 50 000 runs for each point: De Michele's algorithm (circles), the Tao-BD algorithm (plus symbols), a modified Tao-BD algorithm (crosses), Strating's algorithm (diamonds), and a MC algorithm (triangles). For $\Delta t=0.01$, diamonds and circles, as well as crosses and plus symbols overlap. Solid lines are the analytical solutions. The dotted line corresponds to $\exp[-(r_0-\sigma)^2/(4Dt)]/\sqrt{\pi D t}$.

enough Δt; only at unrealistically large step sizes ($\Delta t \gtrsim 1$) does one observe a difference due to "missed" collisions in Starting's algorithm. At this point, however, both algorithms already deviate significantly from the exact solution (shown as a solid line). The convergence to the right solution is good enough to give reasonable results already for $\Delta t=0.1$, about one order of magnitude bigger than what has been used in previous studies.[9–11] For even smaller Δt, also the exact solution becomes indistinguishable from the one-dimensional $\langle \Delta r \rangle_{1D}$, cf. Eq. (10), which can be written (using $\rho_0=r_0-\sigma$) as

$$\langle \Delta r \rangle_{1D} = 2\frac{\sqrt{D\Delta t}}{\sqrt{\pi}} e^{-\rho_0^2/(4D\Delta t)} - \rho_0 \operatorname{erfc} \frac{\rho_0}{\sqrt{4D\Delta t}} \tag{13}$$

for $\rho_0 > 0$ and zero elsewhere.

Let us point out that this convergence is indeed closely related to the elastic-collision rule. In fact, from a Metropolis-MC scheme with Gaussian displacements,[4] one gets the results shown as triangles in Fig. 2. They approach for small Δt their one-dimensional limit $\langle \Delta r \rangle_{1D} = \Theta(\rho_0)\sqrt{D\Delta t/\pi}\exp[-\rho_0^2/(4D\Delta t)]$, dropping a term connected to the possible tunneling of a particle across the excluded-volume region (exponentially small for $\Delta t \ll \sigma^2/4D$). For small ρ_0, this differs from the BD result, Eq. (13), by a factor of 2, highlighting that the approach of MC to true Brownian dynamics is less straightforward even as $\Delta t \to 0$. This can be seen in the lowest panel of Fig. 2; reducing Δt even further will not change the figure, because the 1D asymptote is already reached and exactly scales with $\sqrt{D\Delta t}$ as a function of $\rho_0/\sqrt{D\Delta t}$, as used in the figure. The MC method neglects a term of $\mathcal{O}(\sqrt{\Delta t})$ that is part of the finite-time-step solution of the Smoluchowski equation, whereas De Michele's algorithm has a leading error term of $\mathcal{O}(\Delta t)$, the latter owing to the finite curvature of the particles' boundaries. A similar argument about the convergence of MC to BD has been brought forward by Heyes and Brańka[52] for the case of smooth forces. There, however, one needed to look at the mean-squared displacement $\langle \Delta r^2 \rangle$ to find differences at finite Δt, whereas here the disagreement sets in one level earlier. It also explains why the use of Monte Carlo to simulate BD needed an elaborate density-dependent extrapolation procedure to $\Delta t=0$, using several simulation runs at different $\Delta t > 0$[4].

The algorithm of Tao *et al.*[10] is more difficult to assess analytically. It replaces the deterministic reflection of the extracted trajectories by a stochastic collision law: using as above the fictive velocity to calculate a collision time $0 \leqslant t_c \leqslant \Delta t$, one advances the particles up to contact and then assigns final positions from new random displacements whose variances are in accord with the remaining time $\Delta t - t_c$. The distribution of these secondary displacements has to be restricted such that particles do not recollide. Tao *et al.* state that the displacements should be such that the particles separate initially. If one implements this algorithm for hard disks, the results for $\langle \Delta \mathbf{r} \rangle$ are almost identical to De Michele's ones for large Δt, as the plus symbols in Fig. 2 show. For small Δt, a small but discernible difference seems to remain, owing to the randomness in the velocity reflection. One can introduce a slight modification to the Tao-BD algorithm, in which the postcollision velocities are only required to be such that the two colliding particles do not overlap at the end of the time step. If one does so, one can improve on the result for $\langle \Delta \mathbf{r} \rangle$, as the crosses in Fig. 2 show: for small Δt, this algorithm behaves just like the original Tao-BD one, as expected, and for larger Δt, its results remain closer to the true solution. We did, however, not test this modification for the many-particle case: relaxing the criterion for the postcollision velocities can in principle lead to the same secondary-overlap problems earlier non-ED algorithms suffer from.

B. Many-step behavior

Having discussed the one-step behavior of the algorithms, let us now look at the results after many steps M, i.e., at a time $t=M\Delta t$ large compared to Δt, $M \gg 1$. Here we perform a numerical comparison of the one-particle PDF in the two-dimensional case in the presence of fixed other spheres (corresponding to the relative part of the PDF in the two-body problem). We restrict the discussion to De Michele's algorithm now. As initial condition, let us fix a relative distance $r_0=1.1\sigma$. Since the inversion of the Laplace transformed analytical solution from Refs. 45 and 46 is cum-

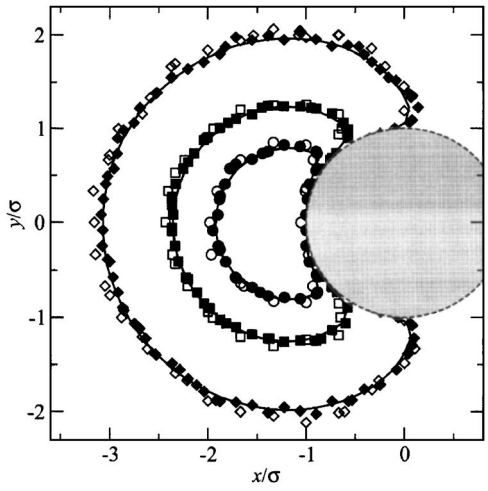

FIG. 3. Contour plot comparing the probability distribution (PDF) for the relative diffusion of two hard spheres (diameter $\sigma=1$, relative diffusion coefficient $D=1$) at time $T=1/4$. Circles (squares, diamonds) are the positions where the binned simulation-data PDF has reached its half-maximum (1/5, 1/50); filled symbols correspond to $\Delta t=0.01$ (5000 steps) and open symbols to $\Delta t=0.1$ (50 steps). Solid lines are the corresponding exact-PDF results. A bin size of $dx=dy=0.32$ was used. The gray circle indicates the position of the second particle (no-flux boundary condition along the dashed line).

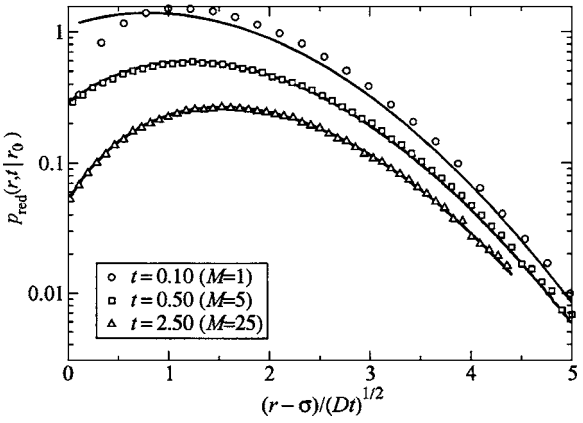

FIG. 4. Two-particle reduced angular preaveraged PDF in three dimensions, $p_{red}(r,t|r_0)$, at times $t=0.1$, 0.5, and 2.5, as a function of the scaled initial separation $(r_0-\sigma)/\sqrt{Dt}$, where $r_0=1.01\sigma$ (solid lines). Results from the De Michele's algorithm with $\Delta t=0.1$ are shown as symbols; they correspond to $M=1$, 5, and 25 simulation time steps.

bersome, we found it easier to obtain the exact PDF numerically. Using Crank's method[53] on a two-dimensional $K\times K$ periodic square mesh ($K=800$) of length $L=8$, conditions of no flux are imposed on a circle; with such conditions Crank's method conserves the probability. Indicating with $\delta x=L/K$, Crank's method is stable for time steps $D\delta t\ll\delta x^2$; the integration time step was chosen as $\delta t=10^{-2}\delta x^2/D$, checking that smaller time steps do not improve the accuracy of the numerical solution. The simulation data was obtained from averages over 200 000 runs, then using data binning with $dx=dy=0.32$ for both the simulation data and the numerically solved PDF.

A visual inspection already yields some insight on the quality of the agreement. To this end, we plot equal-probability contour lines corresponding to the 1/2-, 1/5-, and 1/50-maximum values of the PDF. The comparison of the exact result with De Michele's algorithm is shown in Fig. 3. There, solid lines indicate the exact results, while the different symbols represent the results of De Michele's algorithm with different time steps, $\Delta t=0.01$ (corresponding to $M=5000$ steps) and $\Delta t=0.1$ ($M=50$). One recognizes that the algorithm captures all three contour lines rather nicely. The fluctuations visible in the figure are all well within the fluctuations expected for the number of runs used to obtain the average. We therefore conclude that De Michele's algorithm reproduces the BD two-body PDF also in two dimensions.

Also in the three-dimensional (3D) case, this convergence is observed: as noted above, the one-step results for $\langle\Delta\mathbf{r}\rangle$ do not change qualitatively. Comparing the two-body PDF directly requires a huge set of data; here we restrict the discussion to a special case: a simple expression for the two-particle PDF can be obtained if one starts from a spherically symmetric initial distribution, $p(\mathbf{r},0|\mathbf{r}_0)=\delta(r-r_0)/(4\pi r_0^2)$. The exact form of this reduced angular-symmetric PDF, $p_{red}(r,t|r_0)$, is given in Ref. 54 and is compared with simulation results in Fig. 4. We show a cut using $r_0=1.01\sigma$ and a fixed time step $\Delta t=0.1$ in the algorithm. The final time t is varied through the number of simulation time steps M. Note that this Δt, as judged from Fig. 2, is already quite large, so that for only one simulation time step, a discrepancy is clearly visible. This however vanishes quite quickly; already for $M\approx 5$ the deviations are minute, and for $M\approx 25$, they are no longer identified. Generally, this indicates that the transition from two to three dimension in the analysis of the algorithm poses no surprises. Furthermore, even if in the one-step comparison some differences remain for moderately large Δt, the results obtained after $M\gg 1$ steps can still be correct. We will discuss the implications of this finding in the following section.

V. MANY-BODY TESTS

Let us now turn to a test of the many-body behavior of the algorithm. Having shown that the ED-BD procedure converges to the true PDF after a reasonable number of time steps in the two-body case, the following section demonstrates that this convergence is not destroyed, even if collisions with several particles take place within a few time steps. For high-density HS-BD systems, analytical results are scarce, so we will now restrict the discussion to the three-dimensional mean-squared displacement (MSD), $\delta r^2(t)=\langle(\mathbf{r}(t)-\mathbf{r}(0))^2\rangle$ starting from an equilibrated initial configuration. For the test of De Michele's algorithm, we used $N=1000$ particles at two different volume fractions $\phi=0.05$ (representing the two-body dominated dilute case) and $\phi=0.45$ (where higher-order terms in ϕ are significant).

First, we investigate the low-density limit where one expects that the system is dominated by two-body interactions. Analytical results based on the two-body exact solution are in fact available for the long-time diffusion coefficient $D_L=\lim_{t\to\infty}\delta r^2(t)/(6D_0t)$. To first order in the number density, one gets[45] $D_L=D(1-2\phi)$, where $\phi=(\pi/6)n\sigma^3$ is the packing fraction, and n the number density of the hard-sphere system.

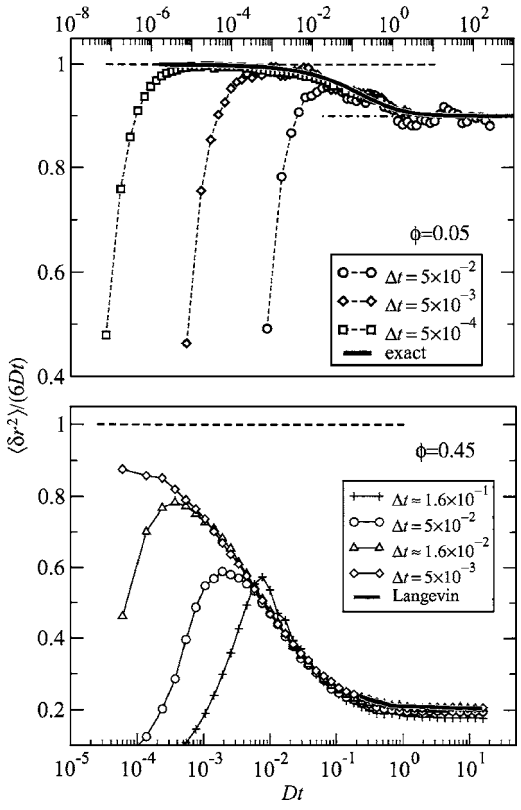

FIG. 5. Mean-squared displacement $\langle \delta r^2 \rangle$ of Brownian hard spheres at packing fractions $\phi=0.05$ (upper panel) and $\phi=0.45$ (lower panel), normalized by the free diffusion limit $6Dt$. Symbols are simulations with De Michele's algorithm using 1000 particles with various step sizes Δt as indicated in the figure. The dashed horizontal line indicates the Brownian-dynamics short-time asymptote, $d(t)=\langle \delta r^2 \rangle/(6Dt)=1$. The dot-dashed line corresponds to the long-time asymptote evaluated to first order in the packing fraction, $d(t)=1-2\phi$. The thick solid line in the upper panel is the exact Brownian-dynamics result (from Ref. 55); in the lower panel, it shows the results from a Langevin simulation with $m/\xi=0.01$ (see text for details).

In the same limit, the full time dependence of the MSD is known analytically up to numerical integration over a (known) memory kernel.[55]

The algorithm's results for the MSD are shown as symbols in Fig. 5, normalized to the free diffusion asymptote, $d(t)=\langle \delta r^2 \rangle/(6Dt)$. For $\phi=0.05$, shown in the upper panel, the low-density long-time asymptote $d(t)=1-2\phi$ is reached for $Dt \gtrsim 1$ for all shown step sizes Δt. In addition, the simulation results for different Δt collapse for $t \gtrsim 5\Delta t$ onto the exact $d(t)$ obtained from Ref. 55 which is shown as a thick solid line in the figure. In agreement with the discussion above (cf. Fig. 4), the algorithm needs about $\mathcal{O}(5)$ steps in order to reproduce correctly the Brownian-dynamics MSD. The effect of the finite step size is clearly seen at short times, $\Delta t \lesssim 0.05$, where the ballistic subintervals in the algorithm lead to a MSD quadratic in time, i.e., $d(t) \sim t$. If one is interested in short time scales, one needs to reduce the time step to $\Delta t=\mathcal{O}(10^{-3})$ in order to recover a window in which the proper Brownian *short-time* dynamics is visible. Otherwise, the artificial ballistic $d(t)$ crosses over directly to the correct *long-time* behavior, at least for realistic (not too big) choices of Δt. It is reassuring that the improper treatment of the short-time dynamics does not influence the convergence to the correct long-time dynamics, and does not even induce an effective time scale (or an effective free diffusion coefficient). In other words, if one is not interested in very early times, a reasonably large Δt can be chosen to obtain the dynamics at $t \gg \Delta t$. This is a clear advantage over other schemes, in which an elaborate $\Delta t \to 0$ extrapolation needed to be applied. For example, in the MC algorithm we find reasonable agreement for $d(t)$ when Gaussian displacements of variance $\delta r^2=\mathcal{O}(0.01\sigma)$ per Cartesian coordinate are chosen. Since in each MC step, a trial move for a single particle is made, this displacement size is connected to a time step by $\delta r^2=2ND\Delta t^4$. For our system, $N=1000$, corresponding hence to a time step $\Delta t \ll 10^{-7}$ in our units.

The regime in which the hard-sphere system is a conceptually and practically relevant reference system corresponds to high volume fractions, e.g., close to the glass transition. Since monodisperse hard spheres crystallize at very high densities, we limit the discussion to $\phi=0.45$, where the liquid is still the thermodynamically stable state. Note, however, that we could use a multicomponent system to study the liquid at higher densities (as it has been done in Ref. 11), but the effect of polydispersity on the MSD would complicate our discussion here too much. At high densities, the interparticle distance d_{avg} decreases drastically; therefore choosing a $\Delta t \ll d_{\mathrm{avg}}^2/(4D)$ in order to deal with two-body events only could be a severe restriction for the computational efficiency. In order to test the behavior of the ED-BD algorithm, we need to compare with a reliable result for the MSD, which is not available analytically at such high density. We therefore performed a "Langevin simulation" with an algorithm adapted from the one-dimensional case given in Ref. 56, using a thermostat designed to reproduce the correct Langevin equation of motion, Eq. (1). This is achieved at the expense of prohibitively long simulation times (about 100 times longer than the corresponding ED-BD runs discussed here), which render this approach impractical for realistic simulation purposes beyond providing a benchmark curve to test our ED-BD algorithm against. The lower panel of Fig. 5 shows the agreement between this Langevin and De Michele's algorithms for long times at $\phi=0.45$. The Langevin result is only shown for large times, since it uses a finite damping $m/\xi=100$ and therefore does not obey proper Brownian dynamics at short times. The ED-BD curves furthermore show the same scenario already observed in the low-density limit (upper panel): decreasing Δt, one opens an increasing window inside which the short-time diffusion is observed. Again, irrespective of the precision with which the short-time characteristics are reproduced, the long-time behavior of the MSD is correct essentially for $\Delta t \lesssim 0.01$, demonstrating the validity of our algorithm also at high densities.

To demonstrate the reliability of the diffusion coefficients determined from De Michele's algorithm, we compare with data obtained from the MC-like BD algorithm by Cichocki and Hinsen.[4] Those data have been estimated from three simulations with different $\Delta t=\mathcal{O}(10^{-2})$ and an extrapolation to $\Delta t \to 0$. They are shown as circle symbols in Fig. 6. In order to compare with our algorithm, we have chosen the same system sizes (between $N=300$ and $N=580$ particles) and a $\Delta t=0.01$ that is of the same order as the Δt used in Ref. 4, but no extrapolation procedure (saving a factor of 3 in

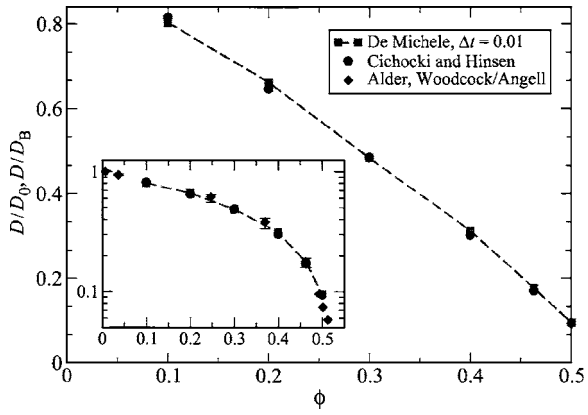

FIG. 6. Comparison of long-time diffusion coefficients as a function of packing fraction $D(\varphi)$, obtained from the present ED-BD algorithm with $\Delta t=0.01$ (squares connected by dashed lines) with those estimated by a $\Delta t \to 0$ extrapolation from the MC algorithm by Cichocki and Hinsen (circles, Ref. 4). The inset shows the same data on a semilogarithmic scale, together with results from Newtonian-dynamics simulations of hard spheres (diamonds, Refs. 57 and 58). The BD data has been normalized by D_0, and the ND data by the Enskog diffusion coefficient D_B.

computing time). The data agree within error bars, underlining the validity of our approach even at finite $\Delta t > 0$.

In fact, the agreement at large densities is perhaps less surprising: there, the long-time dynamics is dominated by collective steric hindrance of the hard spheres, less than by the diffusive nature of the short-time dynamics. This is demonstrated in the inset of Fig. 6, where we show the same data on a semilogarithmic scale, together with diffusion coefficients obtained from Newtonian-dynamics (ND) simulations of hard spheres.[57,58] The latter have been normalized by their low-density limit, viz., the Boltzmann diffusion coefficient, $D_B=(3/8\sqrt{\pi})\sqrt{k_BT/m}/(n\sigma^2)$. Normalized in this form, all data points collapse within error bars onto the same curve $\tilde{D}(\phi)$. At the highest densities, the n dependence of D_B could even be neglected without significant difference. The agreement underlines a well-known fact that the long-time dynamics of dense fluids is, up to a shift in time scales, independent on the specifics of the short-time dynamics.[59]

VI. CONCLUSIONS

We have discussed schemes to integrate the Brownian motion of a many-body hard-sphere system, where the singular potential prevents the use of standard Brownian dynamics techniques dealing with smooth forces. Emphasis was placed on testing their correctness for small but finite integration time steps Δt. We have employed a set of tests based on the exactly known two-particle probability distribution functions for hard spheres.[45,46] These tests are sensitive to both the proper implementation of free diffusion, i.e., the random force in the Langevin equation, Eq. (3), and to the treatment of hard-core "collisions," i.e., the singular hard-sphere force $\mathbf{f}^p$ in this equation. Hence they test both crucial ingredients to the HS-BD problem at low densities. This also guarantees the performance of the algorithm at large densities, where a comparison with ND simulation data shows that collective entropic effects dominate over Brownian motion in the dynamics.

It was shown that De Michele's ED-BD algorithm, that by construction reproduces correctly the statistics of HS systems, indeed converges to the correct solution of Eq. (3). The algorithm works with a finite time step and performs a Newtonian-dynamics simulation within each interval Δt, where the fictive masses of the particles play the role of the inverse diffusion coefficients. Every Δt, random uncorrelated fictive Maxwellian velocities are assigned to each particle, used as a book-keeping device to implement MC-like random moves without overlaps. Such scheme realizes the overdamped limit to the Langevin equation. We have seen that the two main approximations in this scheme are the treatment of particle boundaries as locally flat and the neglect of certain aspects of correlated three-body motion on short time scales. Both of them are well under control for reasonably small but finite Δt.

Unlike a number of earlier schemes (cf. Ref. 9 and citations therein), this ED-BD method avoids unphysical hard-sphere overlaps in any case. Methods based on soft-sphere approximations to the hard-sphere potential either require the use of very small integration time steps or a careful mapping between the structure of hard and soft spheres. Monte Carlo methods, implementing hard-core exclusion but not flux reflection, reproduce Brownian dynamics strictly only for $\Delta t \to 0$. In contrast, by implementing the no-flux boundary conditions correctly to first order in Δt, De Michele's algorithm works reliably with significantly larger time steps. Their magnitude is not bound by the steepness of the potential, but only by the size of the hard spheres. The dynamical features of Eq. (3) are correctly reproduced after a small number of such time steps, and the method is stable in the sense that no drift or effective rescaling is introduced to the long-time behavior when increasing the step size within the limits named above. This is an improvement over methods requiring careful extrapolation to $\Delta t \to 0$. Note that in continuous-potential methods, the time step Δt plays a different role, since it needs to be small enough to ensure the correct integration of the equations of motion, even without Brownian motion. In our case, Δt is essentially a tool to incorporate randomness.

As a simple extension of well-tested event-driven methods for hard spheres, De Michele's algorithm shares their effectiveness (but also the problem of being difficult to parallelize). The same holds for the method recently developed by Tao *et al.*,[10] although the latter is somewhat more expensive in terms of computing time: there, considerably more random numbers need to be drawn (at least one more per collision and dimension), while De Michele's algorithm uses simpler velocity-reflection laws. We found no considerable difference concerning the results between the two methods, but De Michele's ED-BD algorithm is easier to discuss analytically, as it is formally equivalent to a hybrid Monte-Carlo scheme.

De Michele's algorithm can easily be extended from the equilibrium case tested here. We have discussed in particular how to include linear shear flows (of in principle arbitrary magnitude). At large shear rate, one needs to take into account two modifications, namely, a deterministic drift and a distortion of the fictive-velocity distribution. The latter has so far been ignored in the discussion of BD-HS algorithms.

Further extensions such as the inclusion of finite inertial terms, or of finite stepwise interactions, will be discussed in subsequent publications.

ACKNOWLEDGMENTS

The authors acknowledge support from MIUR-Firb and Cofin. They thank M. Fuchs for useful discussion and F. Sciortino for his ongoing support. One of the authors (Th.V.) thanks for the hospitality at the Dipartimento di Fisica of Università di Roma "La Sapienza" where this research has been started and for funding from the Deutsche Forschungsgemeinschaft, DFG Vo 1270/1-1.

[1] D. L. Ermak, J. Chem. Phys. **62**, 4189 (1975).
[2] J. P. Hansen and I. R. McDonald, *Theory of Simple Liquid*, 2nd ed. (Academic, New York, 1989).
[3] P. N. Pusey, in *Liquids, Freezing and Glass Transition*, edited by J. P. Hansen, D. Levesque, and J. Zinn-Justin (North-Holland, Amsterdam, 1991), pp. 765–942.
[4] B. Cichocki and K. Hinsen, Physica A **166**, 473 (1990).
[5] D. M. Heyes and J. R. Melrose, J. Non-Newtonian Fluid Mech. **46**, 1 (1993).
[6] I. Moriguchi, K. Kawasaki, and T. Kawakatsu, J. Phys. II **5**, 143 (1995).
[7] W. Schaertl and H. Sillescu, J. Stat. Phys. **74**, 687 (1994).
[8] D. R. Foss and J. F. Brady, J. Fluid Mech. **407**, 167 (2000).
[9] P. Strating, Phys. Rev. E **59**, 2175 (1999).
[10] Y.-G. Tao, W. K. den Otter, J. K. G. Dhont, and W. J. Briels, J. Chem. Phys. **124**, 134906 (2006).
[11] G. Foffi, C. D. De Michele, F. Sciortino, and P. Tartaglia, Phys. Rev. Lett. **94**, 078301 (2005), where the algorithm used is incorrectly called Strating's.
[12] F. de Jesús Guevara-Rodríguez and M. Medina-Noyola, Phys. Rev. E **68**, 011405 (2003).
[13] Mathias Fuchs (private communication).
[14] J. F. Brady, J. Chem. Phys. **98**, 3335 (1993).
[15] J. F. Brady and G. Bossis, Annu. Rev. Fluid Mech. **20**, 111 (1988).
[16] A. J. C. Ladd, J. Fluid Mech. **271**, 285 (1994).
[17] A. J. C. Ladd and R. Verberg, J. Stat. Phys. **104**, 1191 (2001).
[18] M. E. Cates, K. Stratford, R. Adhikari, P. Stansell, J.-C. Desplat, I. Pagonabarraga, and A. J. Wagner, J. Phys.: Condens. Matter **16**, S3903 (2004).
[19] R. Adhikari, K. Stratford, M. E. Cates, and A. J. Wagner, Europhys. Lett. **71**, 473 (2005).
[20] P. J. Hoogerbrugge and J. M. V. A. Koelman, Europhys. Lett. **19**, 155 (1992).
[21] R. D. Groot and P. B. Warren, J. Chem. Phys. **107**, 4423 (1997).
[22] H. Tanaka and T. Araki, Phys. Rev. Lett. **85**, 1338 (2000).
[23] Y.-G. Tao, W. K. den Otter, and J. T. Padding, J. Chem. Phys. **122**, 244903 (2005).
[24] S. Duane, A. D. Kennedy, D. Pendleton, and B. J. Roweth, Phys. Lett. B **195**, 216 (1987).
[25] D. B. Mehlig, D. W. Hermann, and B. M. Forrest, Phys. Rev. B **45**, 679 (1992).
[26] M. P. Allen and D. J. Tildesley, *Computer Simulation of Liquids*, 2nd ed. (Clarendon, Oxford, 1987).
[27] P. E. Kloeden and E. Platen, *Numerical Solution of Stochastic Differential Equations*, Applications of Mathematics Vol. 23, 3rd ed. (Springer, New York, 1999).
[28] W. Xue and G. S. Grest, Phys. Rev. Lett. **64**, 419 (1990).
[29] P. Turq, F. Lantelme, and L. Friedman, J. Chem. Phys. **66**, 3039 (1977).
[30] E. Helfand, J. Chem. Phys. **69**, 1010 (1978).
[31] A. Iniesta and J. García de la Torre, J. Chem. Phys. **92**, 2015 (1990).
[32] R. Honeycutt, Phys. Rev. A **45**, 600 (1992).
[33] A. C. Brańka and D. M. Heyes, Phys. Rev. E **58**, 2611 (1998).
[34] R. D. Skeel and J. A. Izaguirre, Mol. Phys. **100**, 3885 (2002).
[35] W. Wang and R. D. Skeel, Mol. Phys. **101**, 2149 (2003).
[36] A. Ricci and G. Ciccotti, Mol. Phys. **101**, 1927 (2003).
[37] D. Kannan and V. Lakshmikantham, *Handbook of Stochastic Analysis and Applications* (Marcel Dekker, 2002).
[38] D. C. Rapaport, *The Art of Molecular Dynamics Simulation* (Cambridge University Press, Cambridge, 2004).
[39] M. Allen, D. Frenkel, and J. Talbot, Comput. Phys. Rep. **9**, 301 (1989).
[40] S. Luding, H. J. Herrmann, and A. Blumen, Phys. Rev. E **50**, 3100 (1994).
[41] S. Luding, Phys. Rev. E **52**, 4442 (1995).
[42] D. R. M. Williams and F. C. Mackintosh, Phys. Rev. E **54**, 9 (1996).
[43] G. Peng and T. Ohta, Phys. Rev. E **58**, 4737 (1998).
[44] T. P. C. van Noije, M. H. Ernst, E. Trizac, and I. Pagonabarraga, Phys. Rev. E **59**, 4326 (1999).
[45] S. Hanna, W. Hess, and R. Klein, Physica A **111**, 181 (1982).
[46] B. J. Ackerson and L. Fleishman, J. Chem. Phys. **76**, 2675 (1982).
[47] A. D. Polyanin, *Handbook of Linear Partial Differential Equations for Engineers and Scientists* (CRC, Boca Raton, FL, 2002).
[48] R. A. Lionberger and W. B. Russel, J. Rheol. **38**, 1885 (1994).
[49] R. T. Foister and T. G. M. van de Ven, J. Fluid Mech. **96**, 105 (1980).
[50] R. Courant and D. Hilbert, *Methods of Mathematical Physics* (Wiley, New York, 1953), Vol. I.
[51] P. P. Valkó and J. Abate, Comput. Math. Appl. **48**, 629 (2004); MATHEMATICA source code from http://library.wolfram.com/infocenter/MathSource/4738/
[52] D. M. Heyes and A. C. Brańka, Mol. Phys. **94**, 447 (1998).
[53] J. Crank, *The Mathematics of Diffusion*, 2nd ed. (Clarendon, Oxford, 1975).
[54] K. Schulten and I. Kosztin, *Lectures in Theoretical Biophysics* (University of Illinois at Urbana-Champaign, Urbana, IL, 2000), http://www.caam.rice.edu/~cox/stoch/lectheobio.pdf
[55] H. N. W. Lekkerkerker and J. K. G. Dhont, J. Chem. Phys. **80**, 5790 (1984).
[56] B. G. de Grooth, Am. J. Phys. **67**, 1248 (1999).
[57] B. J. Alder, D. M. Gass, and T. E. Wainwright, J. Chem. Phys. **53**, 3813 (1970).
[58] L. V. Woodcock and C. A. Angell, Phys. Rev. Lett. **47**, 1129 (1981).
[59] T. Geim, W. Kob, and K. Binder, Phys. Rev. Lett. **81**, 4404 (1998).